Embedded cluster density functional and second-order Møller-Plesset perturbation theory study on the adsorption of N_2 on the rutile (110) surface

Dorothee Stodt* and Christof Hättig†

Department of Theoretical Chemistry, Ruhr-Universitaet Bochum

(Dated: August 20, 2012)

Abstract

The adsorption of N_2 on the rutile TiO_2 (110) surface in the limit of low coverage has been studied as a prototype example for the adsorption of non-polar molecules on strongly ionic oxide surfaces. We employed for this study an embedded cluster ansatz in combination with density functional theory and wavefunction methods. Both, clusters saturated with hydrogen atoms and electrostatically embedded clusters have been applied and methods and basis sets have been varied to test their reliability and accuracy for describing the electrostatic potential on the surface and its interaction with the non-polar N_2 molecule. Quantum clusters consisting of up to 342 atoms have been used to converge the results with respect to the cluster size. For electrostatically embedded clusters the convergence can considerably be enhanced by optimizing the charges for the point charge embedding. On the rutile (110) surface an accurate account of the long ranging interaction of the adsorbate with the bridging oxygen atoms is important for quantitative adsorption energies of weakly bound molecules. In addition the geometric relaxation of the surface has a marked influence on the results, whereas the basis set–dependence of the electrostatic potential is small. Of all methods investigated (HF, DFT/PBE, DFT/B3LYP, MP2), only MP2 and DFT/B3LYP were able to describe the adsorption of N_2 on the rutile surface properly. After including the zeropoint vibrational energy the calculated adsorption energy is close to experimental results. The approach is thus promising for future investigations on adsorption energies and structures of non-polar molecules on ionic oxide surfaces.

*Electronic address: dorothee.stodt@rub.de

†Electronic address: christof.haettig@rub.de

I. INTRODUCTION

The adsorption of molecules on the TiO_2 surfaces is an intensively studied subject. [1–4] Chemisorption is often already correctly described by computationally cheap semi-local density functional theory (DFT), e.g. with generalized gradient approximation (GGA) functionals. An accurate description of the weak interaction between a physisorbed species and a surface is very demanding for electronic–structure methods. The physisorption of the non-polar N_2 molecule, which does not possess a dipole moment and is chemically almost inert is a prototypical example for this. First quantum chemical investigations on the adsorption of N_2 on the TiO_2 surface were carried out in 1998 by Rittner *et al.* [5], who later also calculated a potential energy surface for this interaction.[6] These calculations, however, were limited by the computational possibilities available 14 years ago. Due to better hardware and improved algorithms and approximations it is today possible to do calculations for larger model systems and to account more accurately on correlation effects which play an important role for physisorption. One aim of this study has been to develop a work flow for future quantum mechanical investigations on the physisorption of molecules on the rutile (110) surface. In physisorbed systems the binding depends on weak interactions such as electrostatic, induction and the ubiquitous van der Waals dispersion interactions. In particular the dispersion interaction which is a non-local electron correlation effect is demanding for electronic–structure methods. The Hartree-Fock self-consistent field (HF-SCF) method, based on a mean field approximation for the electron repulsion, does not include it at all. DFT with the common efficient local density approximation (LDA), GGA, and hybrid type functionals includes only local correlation effects and, thus, do not correctly account for the non-local dispersion interaction. Correlated wave function based methods such as configuration interaction (CI), coupled cluster (CC) or Møller-Plesset perturbation theory (MPPT) include dispersion interaction as part of the correlation energy, but are computationally much more involved and therefore limited to smaller systems.

There are mainly two concepts used to account for long range interactions between an adsorbate and the surface of a condensed phase. With periodic boundary conditions a unit cell, which is a small cut-out of the surface is infinitely repeated. In the regime of low coverage large super cells of the true surface unit cell can be used to minimize unwanted lateral interactions between adsorbates. Depending on the method there are several programs avail-

able. This approach is in particular often used in combination with semi-local GGA density functionals as many efficient periodic DFT implementations are available. Periodic implementations of second-order Møller-Plesset perturbations theory (MP2) have been developed by Schütz and coworkers [7] and also by Marsman *et al.* [8]. Also a periodic implementation of CCSD is available e.g. in the VASP package [9, 10]. The computational demands for such calculations are, however, extremely high. A computational simplification of periodic boundary conditions is the cyclic cluster approach developed by Bredow *et al.* [11].

An alternative approach is to model the surface by finite clusters. Compared to periodic calculations, finite cluster approaches have to deal with boundary effects not only in one but in three directions. To minimize them and improve convergence with cluster size they are often embedded in a potential to account for long ranging electrostatic interactions or saturated at the boundaries with capping atoms to avoid artifacts from dangling bonds. Which kind of embedding is more appropriate depends on the ionic or covalent character of the system modeled. We aim at investigations in the limit of low coverage which is in particular important for studying defects and the catalysis of reactions by interaction with the surface. In this regime embedded cluster calculations have the advantage that no computational expensive large super cells have to be used. Another important advantage of embedded cluster approaches is that they can easily be combined with any electronic–structure method and code.

For TiO_2 clusters it is not obvious whether a saturation of dangling bonds with e.g. hydrogen atoms as shown in Fig. 1 or an embedding in a point charge field to account for the Madelung potential leads to a better description of the electronic structure. The bonds in TiO_2 are strongly ionic, but modeling it with Ti^{4+} and O^{2-} ions would clearly overemphasize the ionicity. This raises for an electrostatic embedding the question which charges should be used for a point charge field. Another question we address in this work is, how sensitive results for physisorption energies on the rutile (110) surface are to the employed electronic–structure method (HF-SCF, DFT with GGA or hybrid functionals, or the correlated wavefunction method MP2) and the quality of the basis set.

II. COMPUTATIONAL DETAILS

All calculations were carried out using the TURBOMOLE program package [12]. For the HF-SCF calculations we used either the SVP basis sets [13] for all atoms or a combination of TZVPP [14] for the adsorption center and its nearest neighbors (N_2 and the closest 9 Ti and 15 O atoms) with SVP for all other atoms. All RI-DFT calculations[15] were carried out with the SVP basis[16], while, due its larger basis set demands, we used the combination of either TZVPP and SVP or QZVP[17] and TZVP[18] for the MP2 and SCS-MP2[19] calculations. The latter have been carried out with the parallel RI-MP2 implementation described in Ref. [20] using the optimized SVP[14], TZVP[14], TZVPP[14] and QZVP[21] auxiliary basis sets. In these calculations the $1s^2$ and $2s^22p^6$ shells of the Ti and the $1s^2$ shells of the O and N atoms were kept frozen at the MP2 level. DFT calculations were carried out with the PBE[22–25] and B3LYP[22, 23, 26–28] functionals. For comparison we evaluated for the $Ti_{40}O_{80}$ cluster at the equilibrium structure optimized at the B3LYP level a dispersion energy correction to the DFT energy with the DFT-D3 potential developed by Grimme and coworkers[29]. For the electrostatically embedded clusters the positive point charges closest to the quantum clusters (97 for Ti_5O_{10}, 264 for Ti_9O_{18}, 219 for $Ti_{40}O_{80}$, 408 for $Ti_{96}O_{192}$, and 247 for $Ti_{114}O_{228}$) have been augmented with an effective Ca^{2+} core potential from Ref. [30] to account for the Pauli repulsion of the titanium cations which have a similar radius. In order to minimize the error due to a limited basis set, all results are counterpoise corrected.

III. PERFORMANCE OF THE EMBEDDING SCHEMES FOR TIO_2

To test the performance of hydrogen-saturated and electrostatically embedded clusters and to determine the optimal charges for the latter we followed a similar approach as in Ref. [5] and did for each scheme a series of HF-SCF/SVP calculations for clusters of increasing size. Since the charges of the Ti and O atoms in TiO_2 are not well defined all clusters were chosen such that they are electrically neutral. Furthermore, they have been build symmetrically around the central titanium atom to which the N_2 molecule binds. The Ti-O bond distances were fixed at the bulk values of 1.981 Å and 1.948 Å reported by Restori *et al.* [31].

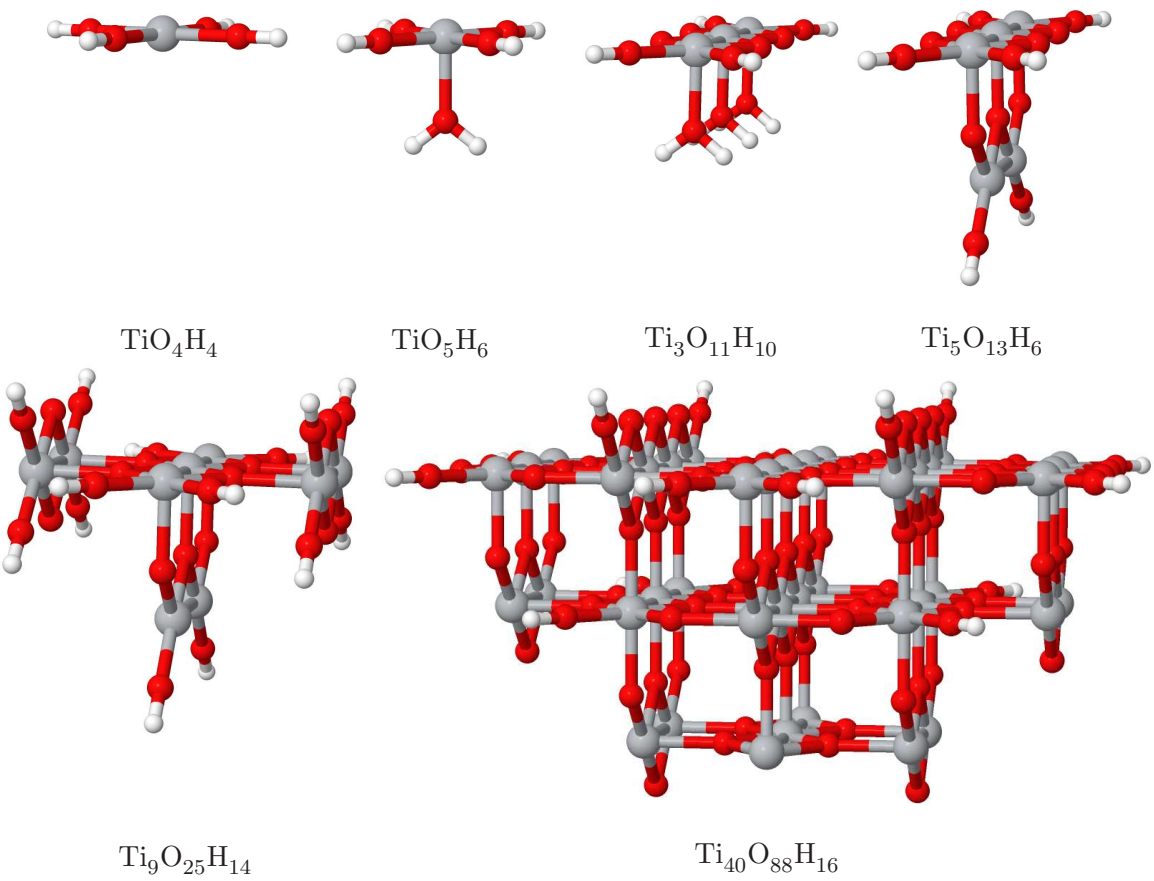


FIG. 1: Structures of the six hydrogen-saturated clusters TiO_4H_4, TiO_5H_6, $Ti_3O_{11}H_{10}$, $Ti_5O_{13}H_6$, $Ti_9O_{25}H_{14}$ and $Ti_{40}O_{88}H_{16}$. The adsorption center of the perpendicular N_2 adsorption is always located in the middle of the cluster.

We used for this study six hydrogen-saturated clusters shown in Fig. 1. The structures for TiO_4H_4, TiO_5H_6, $Ti_3O_{11}H_{10}$, and $Ti_9O_{25}H_{14}$ have been taken from Ref. [5]. To this series we added two new clusters, $Ti_5O_{13}H_6$ and $Ti_{40}O_{88}H_{16}$, build according to the same principles and using the same O-H distance. Fig. 2 shows the five electrostatically embedded clusters used in this study. The structure of Ti_9O_{18} is similar to the largest embedded cluster used by Rittner *et al.* [5]. To this cluster we added for the convergence study one smaller (Ti_5O_{10}) and three larger clusters ($Ti_{40}O_{80}$, $Ti_{96}O_{192}$, and $Ti_{114}O_{228}$).

For both series of clusters we calculated at the HF-SCF level a potential energy curve for the perpendicular adsorption of N_2 as function of the Ti-N distance with the N-N bond distance fixed at the experimental equilibrium distance of 1.098 Å [32]. The final values for the Ti-N bond distances and binding energies have been determined by interpolating between the three energetically lowest points with a quadratic function.

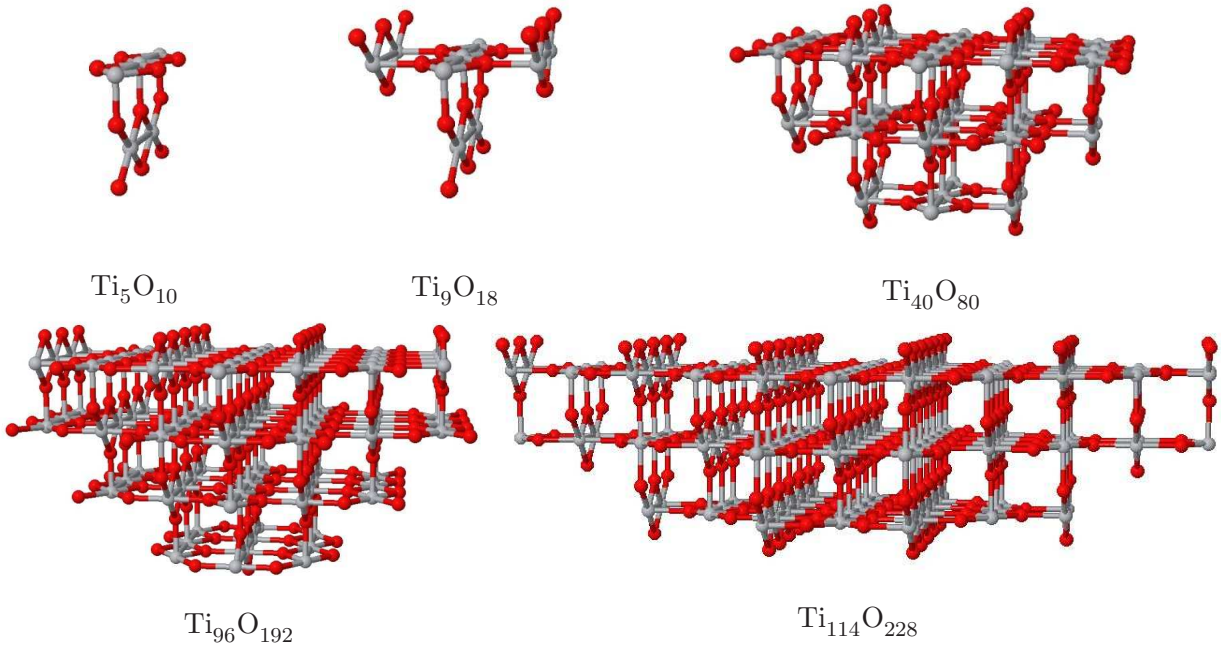


FIG. 2: Structures of the five electrostatically embedded clusters Ti_5O_{10}, Ti_9O_{18}, $Ti_{40}O_{80}$, $Ti_{96}O_{192}$, and $Ti_{114}O_{228}$. The adsorption center of the perpendicular N_2 adsorption is always located in the middle of the cluster.

A. Hydrogen-saturated clusters

As known from the work of Rittner *et al.* [5], a complete oxygen coordination shell of the Ti atom to which N_2 binds and the interaction of the N_2 molecule with the bridging oxygen atoms, which stick out of the otherwise flat rutile (110) surface, are of utmost importance for a qualitatively correct adsorption potential. Both effects are clearly visible in the results for the bond distances and binding energies shown in Fig. 3: Saturating the coordination shell of the Ti atom from TiO_4H_4 to TiO_5H_6 leads to a decrease of the binding energy by more than 10 kJ/mol and adding a first shell of neighbor rows with bridging oxygen atoms, which is the only difference between the clusters $Ti_5O_{13}H_6$ and $Ti_9O_{18}H_{14}$, increases the binding energy by almost 25 kJ/mol. But also a further extension of the cluster model to $Ti_{40}O_{88}H_{16}$ changes visibly the bond distance and decreases the binding energy by 6 kJ/mol, although not yet including second neighbor rows with bridging oxygen atoms, which can be expected to have an even larger influence. Considering these changes in the bond distance and binding energy, it is obvious, that it will be rather difficult to reach converged results with hydrogen-saturated clusters.

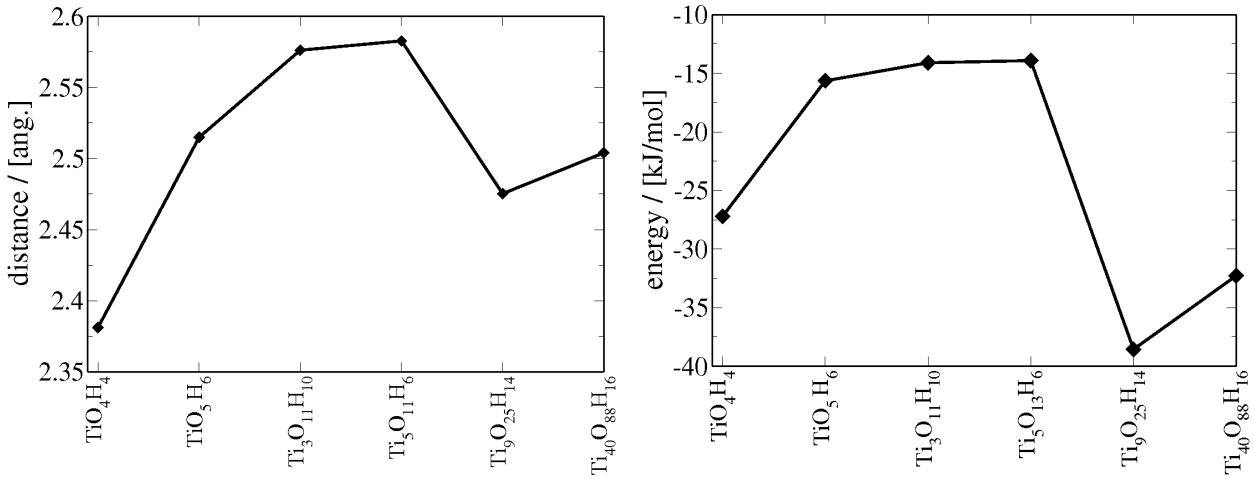


FIG. 3: Convergence study with hydrogen-saturated cluster models. Left part: change of the N-Ti bond distance with cluster size. (The N-Ti bond distance is measured from the central Ti atom and the closest N atom.) Right part: change of the adsorption energy with cluster size.

Nevertheless, the difference between the Ti-N bond distances for the varying clusters is not very large (Fig. 3). They fluctuate between 2.4 Å and 2.6 Å and their change with the cluster size correlates with the change in the binding energy.

B. Electrostatically embedded clusters

For the embedded cluster calculations we used the periodic electrostatic embedded cluster method (PEECM) developed by Burow *et al.* [33]. In these calculations the total system is split into two parts: A fully quantum mechanically treated inner quantum cluster and a long part which is modeled as periodic array of point charges. To avoid artefacts due to an unphysical attraction of electrons by bare positive point charges, the two closest shells of titanium cations around the quantum cluster are modeled with effective core potentials, representing the core electrons of the cations. The electrostatic interaction between the quantum cluster and the infinite point charge array is evaluated in PEECM with the periodic fast multipole method[34].

For calculations on surfaces the point charge array is a two-dimensional slap with a finite thickness. The interaction of the TiO quantum cluster with a N_2 molecule converges, however, quickly with the number of layers in the point charge slap as is seen from the results listed in Tab. I for the adsorption energy of N_2 on the embedded TiO_4 cluster at the

TABLE I: Convergence of the adsorption energy of N_2 on the TiO_4 cluster with the thickness d_z of the periodic point charge slap. ΔE_{ad} is the deviation of the adsorption energy from a reference result calculated with 14 TiO_2 layer thick slap. The results have been obtained at the HF-SCF/SVP level with ionic charges of +4.0 and −2.0 for the embedding potential.

number of TiO_2 layers	d_z [Å]	ΔE_{ad} [kJ/mol]
2	6.95	+0.96
3	9.74	−0.06
4	12.99	−0.01

HF-SCF/SVP level. Already with 3 layers the result is converged within 0.1 kJ/mol. To be on the save side and to have a slap which can also be used with the larger clusters, we used for the following calculations always 8 layers.

More problematic are the Madelung charges for the embedding potential. To find the optimal charges for the embedding, we studied the convergence of the N-Ti bond distance and the adsorption energy at the HF-SCF/SVP level with the cluster size in the series Ti_5O_{10}, Ti_9O_{18}, $Ti_{40}O_{80}$, $Ti_{96}O_{192}$, and $Ti_{114}O_{228}$ and varied the charge of the titanium cations in steps of 0.25 between +2.0 and +4.0 with the charge of the anions set to minus half the cation charge. The results are shown in figure 4. Charges between +2.75 and +3.0 for the titanium cations and −1.375 and −1.5 for the oxygen anions lead to the fastest and most smooth convergence of the results. These are somewhat larger charges than found in Ref. 5 as optimal values for the Madelung charges. For simplicity we choose for the following charges of +3.0 for the cations and −1.5 for the anions.

From Fig. 4 it is also apparent, that in particular the adsorption energy changes at the beginning stepwise with prominent changes when new rows of protruding bridging oxygens are added at the surface from the Ti_5O_{10} to the Ti_9O_{18} and from the $Ti_{40}O_{80}$ to the $Ti_{96}O_{192}$ cluster. First beyond the latter cluster we don't observe a further step. That the bridging oxygen atoms are important for the adsorption energy of N_2 on the rutile (110) surface was already noticed by Rittner *et al.* in Ref. 5, where they tested the hypothesis that the adsorption energy is largely determined by the layers of bridging oxygen atoms by comparing the results for the Ti_9O_{18} cluster shown in Fig. 2 with those from a Ti_9O_{18} cluster with a so

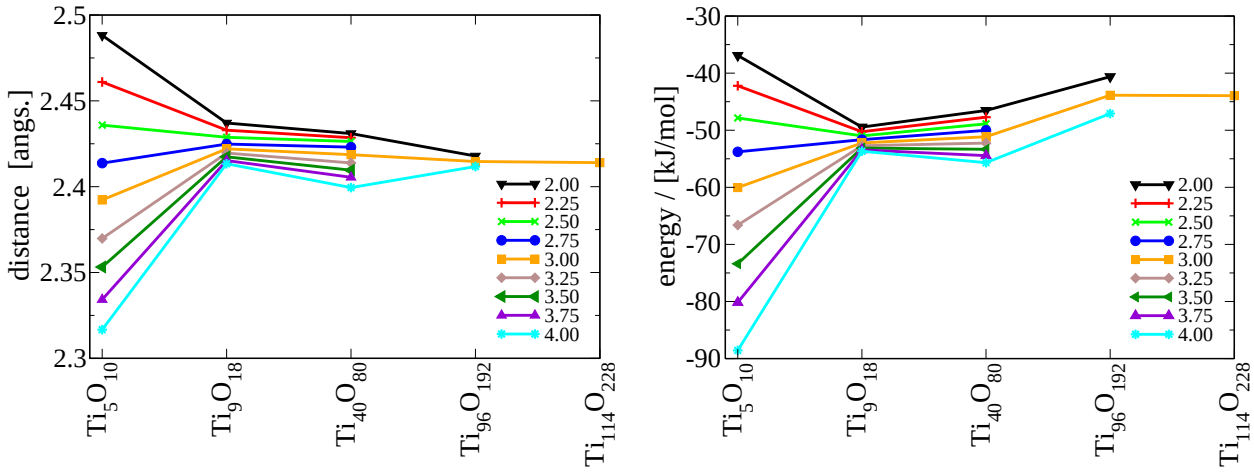


FIG. 4: Convergence studies with electrostatically embedded clusters with the charges of the Ti cations varied in steps of 0.25 between +2.0 and +4.0. The charge of the O anions was always set to minus half the charge of the Ti cations. On the left: convergence of the N-Ti bond distance with the cluster size. On the right: convergence of the binding energy.

called "inverted" geometry, shown in Fig. 5, where the protruding bridging oxygen atoms have been replaced by point charges and ECPs, while the quantum chemically described oxygen atoms are located below the Ti layer. With this cluster model the adsorption energy of N_2 is largely overestimated: With the current basis sets and Madelung charges the HF-SCF result for E_{ad} is -64.7 kJ/mol and almost 12 kJ/mol larger than with the regular Ti_9O_{18} cluster. It deviates from the result with the largest $Ti_{114}O_{228}$ cluster even more than the result obtained with the same Madelung charges for the small Ti_5O_{10} cluster.

With increasing cluster size the adsorption energy becomes slowly less sensitive to the values of Madelung charges. On the $Ti_{96}O_{192}$ cluster the adsorption energies obtained with cationic charges of +2.0 and +4.0 deviate only by $\pm$ 3.2 kJ/mol from the -44.0 kJ/mol obtained with a charge of +3.0 and for the larger $Ti_{114}O_{228}$ cluster the influence of the Madelung potential will be even smaller. Compared to the adsorption energy, the N-Ti bond distance converges more quickly. Already with the Ti_5O_{10} cluster the result (239 pm) agrees within 2 pm with the value for the largest cluster, $Ti_{114}O_{228}$ (241pm).

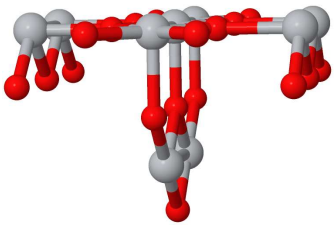


FIG. 5: Ti_9O_{18} cluster with inverted geometry as suggested by Rittner *et al.*[5].

TABLE II: Comparison of the convergence of the adsorption energy and the N-Ti bond distance with the cluster size for H-saturated and electrostatically embedded clusters models with ionic charges of +3.0 and −1.5. The uncertainty in the bond distance and the adsorption energy due to the finite grid for the potential is, respectively, about ±1 pm and 0.2 kJ/mol.

	embedding	Ti_3	Ti_5	Ti_9	Ti_{40}	Ti_{96}	Ti_{114}
E_{ad} in kJ/mol	H-saturated	-14.1	-13.9	-38.6	-32.3		
	PEECM		-60.0	-52.2	-51.1	-43.7	-44.0
$d_{\text{N-Ti}}$ in Å	H-saturated	2.57	2.58	2.47	2.51		
	PEECM		2.39	2.42	2.40	2.41	2.41

C. Comparison of the embedding schemes

Table II shows a comparison of the saturated and periodic embedded cluster model for the binding energy and distance. These results show that the electrostatic embedding leads for the adsorption on the rutile surface to a faster convergence with the size of the cluster model: Already the change in the adsorption energy between the small Ti_5O_{10} and Ti_9O_{18} clusters are with the electrostatic embedding much smaller than with the H-saturated cluster models. One might argue that this result is not very conclusive since the adsorption on the small electrostatically embedded Ti_5O_{10} cluster is extremely sensitive to the values of the Madelung charges. But the same trend is even more clearly seen in the step to the next larger cluster models from the Ti_9 to Ti_{40}, where with electrostatic embedding the adsorption energy changes only by ≈ 1 kJ/mol while it changes by more than 6 kJ/mol between the H-saturated $Ti_9O_{25}H_{14}$ and $Ti_{40}O_{88}H_{16}$ clusters. The N-Ti bond distance is less sensitive to the embedding, but also this property converges with the electrostatic embedding faster.

In summary, it seems that for the interaction of small molecules with the rutile (110) surface the PEECM is superior to H-saturated cluster models, which is slightly different from the findings in Ref. [5] where from the results on smaller clusters it could not be concluded that hydrogen saturation is inferior to an embedding in a Madelung potential. For the subsequent calculations we used therefore exclusively the PEECM with ionic charges of +3.0 and −1.5 as embedding scheme.

In 2010, Ammal *et al.*[35] allready studied the convergence of PEECM embedded clusters with PBE/TZVP for the formal charges of +4.0 for Ti and −2.0 for O. They tested cluster sizes between Ti_9O_{18} and $Ti_{40}O_{80}$ and analyzed the adsorption energy of a platinum atom on the surface. They found in agreement with the current results only a small difference in the adsorption energies obtained with these cluster sizes. These authors also tested the dependence of the results on the charges for the point charge field by doing calculations with reduced charges of +2.0 and −1.0, but eventually recommend to use the formal charges for the embedding, despite a slower convergence of the adsorption energy, since with formal charges the HOMO-LUMO gap agrees better with the band gap in periodic GGA calculations.

However, the band gap problems largely vanishe with hybrid functionals or HF-SCF. Therefore, we decided to use optimized point charges to enhance the convergence with the cluster size for the sensitive N_2-rutile interaction.

IV. INFLUENCE OF SURFACE STRUCTURE RELAXATION AND ELECTRON CORRELATION

A. Surface structure relaxation

In the previous sections we used for the quantum cluster and for the position of the embedding point charges and ECPs fixed geometries obtained as cut-outs from the bulk structure. These models keep the five-fold coordinated Ti centers on the rutile (110) surface fixed in the geometry of a octahedrally coordinated bulk Ti atom and therefore overestimate strongly the adsorption strengths at the surface Ti centers.

To account for the relaxation of the rutile (110) surface we started from an optimized geometry for a TiO_2 slap obtained by Kowalski *et al.*[36] in a periodic plane wave DFT

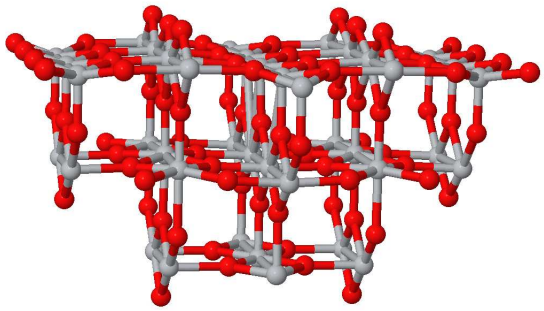


FIG. 6: Geometry of the relaxed $Ti_{40}O_{80}$ quantum cluster.

calculation with the PBE[37] functional. The relaxation of the rutile (110) surface reduces in the uppermost layer the Ti-O bond lengths by about 0.02 Å to 2.006 Å and 1.960 Å and the five-fold coordinated titanium atoms are shifted by about 0.3 Å towards the bulk to increase the strengths of its remaining five Ti-O bonds (see Fig. 6). There are also smaller changes in the other bond lengths and the bond angles. For the details we refer to Ref. 36. For the embedded cluster calculations we used the coordinates from the optimized surface geometry for the periodic point charge embedding, the ECPs and also as start structure for the atoms in a $Ti_{40}O_{80}$ quantum cluster.

We then optimized at the HF/SVP level the positions of the inner atoms in the quantum cluster. Only the positions of those atoms which are directly coordinated to an ECP or a point charge were held fixed. All other atoms of the cluster are allowed to relax and adjust their position to the method and basis set. At the HF/SVP level the so obtained structure for a $Ti_{40}O_{80}$ cluster differs very little from the start structure taken from Ref. 36, which shows that at this level the structure does not depend much on the method and basis set.

Also the adsorption of the N_2 molecule on the surface leads only to very small changes in the geometry of the rutile cluster and the N-N distance, which with 1.07 Å remains also unchanged from the HF/SVP gas phase value (1.07 Å). The N-Ti bond distance on the relaxed surface model is with 2.47 Å somewhat larger than on the unrelaxed cluster model. In line with this, the adsorption energy is with -37.1 kJ/mol on the relaxed $Ti_{40}O_{80}$ cluster about 14 kJ/mol smaller than on the unrelaxed cluster, which demonstrates the importance of the surface relaxation for an accurate description of adsorption properties.

B. Electron correlation effects

To study the importance of electron correlation and remaining basis effects, we used again the $Ti_{40}O_{80}$ cluster with Madelung charges of +3.0 and −1.5. Here, we find with the unrelaxed surface geometry used in Sec. III a strong overestimation of correlation effects. At the DFT level the HOMO-LUMO gap vanishes with the PBE functional almost completely: it is in the SVP basis only ≈ 0.02 eV or 2 kJ/mol. The adsorption energy drops, compared to HF-SCF, by 3.5 kJ/mol to −47.6 kJ/mol. An underestimation of band gaps is a known problem of the PBE functional[38]. For the unrelaxed (110) surface structure the effect becomes exceptionally large due to the inappropriate structure at the undercoordinated five-fold Ti centers. With the hybrid functional B3LYP the HOMO-LUMO gap remains with ≈ 1 eV or 100 kJ/mol larger than with the PBE functional. The B3LYP/SVP result for the adsorption energy on the unrelaxed cluster is with −45.3 kJ/mol almost 5 kJ/mol smaller than with HF-SCF. The most dramatic effect is seen for MP2. For these calculations we replaced the SVP basis set at N_2, the central Ti atom and its nearest O neighbors by the doubly polarized triple-ζ basis TZVPP to account for the larger basis set demands of correlated wave function methods. With this enlarged basis the HF-SCF results for adsorption energy is −49.7 kJ/mol, i.e. 1.4 kJ/mol smaller than in the SVP basis. MP2 predicts for the unrelaxed cluster an unphysically large increase of the adsorption energy due to correlation effects to −68.9 kJ/mol, i.e. an increase by 19.2 kJ/mol or almost 50%. For SCS-MP2 the adsorption energy is with −63.0 kJ/mol just slightly smaller than for regular MP2. The undercoordination of the Ti centers at the fixed bulk geometry leads apparently to strong static correlation effects which are not well described by MP2 and SCS-MP2.

The bond distances for PBE/SVP and B3LYP/SVP differ only very little with 2.41 Å and 2.42 Å from the values obtained with HF-SCF/SVP. For MP2 and SCS-MP2 the distance decreases by 0.07 Å and 0.04 Å, respectively, due to the strong static correlation effects.

With the cluster model for the relaxed (110) surface the correlation effects are considerably smaller. With PBE/SVP the adsorption energy drops with the relaxed structure by about 8 kJ/mol compared to the result obtained with the same functional on the unrelaxed surface and is now −39.8 kJ/mol. B3LYP/SVP gives, after the geometry optimization of the adsorbate and the inner part of the $Ti_{40}O_{80}$ cluster, an adsorption energy of −35.2 kJ/mol,

which is about 2 kJ/mol less attractive than the result obtained with HF-SCF/SVP (−37.1 kJ/mol) . At the B3LYP level we evaluated also the contribution of the monomer deformation energy to the counterpoise correction, which reduces the adsorption energy by about 5.4 kJ/mol. If we account for the dispersion interaction, which is not included in the semi-local B3LYP correlation functional, by means of the empirical D3 dispersion potential[29] we get an additional correction of −29.1 kJ/mol to the binding energy. The difference in the dispersion energy between the minimum geometry of the $Ti_{114}O_{228}$ and $Ti_{40}O_{80}$ cluster yields −0.2 kJ/mol, so that it should be converged with the cluster size. The final result for the B3LYP-D3/SVP adsorption energy is −60.0 kJ/mol.

The MP2 result for the adsorption energy on the relaxed $Ti_{40}O_{80}$ cluster with the TZVPP basis set at the innermost atoms and the SVP basis on all other atoms (as described above) and a geometry optimized with B3LYP/SVP is −58.7 kJ/mol, which is very similar to the dispersion corrected B3LYP-D3 value. With SCS-MP2 the binding energy is again lower than with regular MP2 (−52.2 kJ/mol). An enlargement of the basis set to QZVP for the inner and TZVP for all others atoms leads to an increase of about 4 kJ/mol in the adsorption energy for both MP2 variants. Following, the MP2 and SCS-MP2 binding energies are −64.1 kJ/mol and −56.4 kJ/mol, respectively. To estimate the remaining basis set incompleteness error in the MP2 correlation contribution to the binding energy we extrapolated from the TZVPP/SVP and QZVP/TZVP results the basis set limit with the two point formula proposed by Helgaker *et al.*[39]:

$$E_X = E_{limit} - A \cdot X^{-3} \ , \tag{1}$$

where X is the cardinal number of the basis set, E_X the correlation energy in this basis and E_X the basis set limit of the correlation energy. We used X = 3 for TZVPP/SVP and X = 4 for QZVP/TZVP. The estimated correlation limit for MP2 has been combined with the HF-SCF result for the QZVP/TZVP basis. The resulting estimated basis set limits for the electronic contribution to binding energies are −68.9 kJ/mol and −60.5 kJ/mol for MP2 and SCS-MP2, respectively.

TABLE III: Best estimate for MP2 and SCS-MP2 adsorption energies (in kJ/mol). E_{ad}^{lim} are estimated basis set limits obtained as described in IV B. The correction for incomplete convergence with respect to the cluster size, $E_{ad,Ti_{114}O_{228}}^{DFT/B3LYP}$ -$E_{ad,Ti_{40}O_{80}}^{DFT/B3LYP}$, has been taken from the B3LYP/SVP results on the unrelaxed rutile surface. The ZPVE and the deformation contribution to the counterpoise correction have been evaluated also at the B3LYP/SVP level.

	MP2		SCS-MP2
E_{ad}^{lim} on relaxed $Ti_{40}O_{80}$ cluster	−68.9		−60.5
$E_{ad,Ti_{114}O_{228}}^{DFT/B3LYP} - E_{ad,Ti_{40}O_{80}}^{DFT/B3LYP}$		+9.2	
ZPVE correction		+5.0	
CP deformation correction		+5.4	
Best estimate for E_{ad}	−49.3		−40.9

C. Zeropoint vibrational contribution and comparison with experiment

A non-negligible contribution to the adsorption energy comes in addition from the change of the zero-point vibrational energy (ZPVE) upon adsorption. With B3LYP we obtained on the relaxed $Ti_{40}O_{80}$ cluster in the harmonic approximation an increase of the ZPVE by 5.0 kJ/mol, which is close to the zeropoint vibrational correction of 4.9 kJ/mol found previously in a similar study[40] for the adsorption of CO on the rutile (110) surface.

A correction for the incomplete convergence of the results for the $Ti_{40}O_{80}$ cluster with respect to the cluster size can be obtained from the DFT/B3LYP results with a SVP basis set on the unrelaxed rutile surface (see Secs. III B and III C) as $E_{ad,Ti_{114}O_{228}}^{DFT/B3LYP} - E_{ad,Ti_{40}O_{80}}^{DFT/B3LYP}$ = 9.2 kJ/mol. Adding this correction, the change in the zeropoint vibrational energy upon adsorption (+5.0 kJ/mol), and the contribution from the deformation of the monomers to the counterpoise correction (+5.4 kJ/mol) to the estimated MP2 and SCF-MP2 basis set limits for the pure electronic results on the relaxed $Ti_{40}O_{80}$ cluster, we obtain binding energies of −49.3 and −40.9 kJ/mol for, respectively, MP2 and SCS-MP2. The experimental results for the adsorption energy of N_2 on rutile are −28 and −30 kJ/mol[41, 42]. The former value was recently obtained by Dohnálek *et al.*[42] on a fully oxidized TiO_2 (110) surface at 32 K in the zero coverage limit and the latter result from Furlong *et al.*[41] was determined on powder samples. Taking into account the remaining uncertainties of the experimental and

the calculated binding energies, both values agree reasonably with the final SCS-MP2 result of −40.9 kJ/mol. Unscaled MP2 apparently overestimates the correlation contribution to the binding energy due to strong correlation effects at the undercoordinated Ti centers. The spin-scaled version of second-order perturbation theory is known to be less sensitive to such strong correlation effects.[43] It still overestimates the binding energy, but to a much smaller extend than standard MP2. B3LYP without dispersion correction underestimates with 17.5 kJ/mol the experimental value largely, while with the D3 dispersion correction the result is close to the estimated SCS-MP2 basis set limit. It also overestimates somewhat the binding energy on rutile. This is a known general issue for adsorption energies on ionic surfaces with the standard D3 parameterization, which overestimates the C_6 coefficients for the interaction with Ti atoms in TiO_2[44].

V. SUMMARY AND CONCLUSIONS

We investigated the adsorption of N_2 on the rutile (110) surface with embedded cluster methods using two different embedding schemes and density functional theory as well as spin-component scaled (SCS) and unscaled second-order Møller-Plesset perturbation theory. We find that the binding energy and the bond distance converge considerably faster with electrostatically embedded clusters (PEECM) than with hydrogen-saturated cluster models and recommend PEECM for TiO_2 clusters. A comparison of the convergence rates for cluster sizes between 15 and 342 atoms with different charges for the embedding revealed that charges of +3.0 for the titanium and −1.5 for the oxygen atoms leads to the fastest convergence of the results with the cluster size.

For the adsorption on the rutile (110) surface an accurate description of the interaction between the adsorbate and the bridging oxygen atoms at the surface is crucial. For N_2 it turned out that at least two rows of bridging oxygen atoms on both sides of the adsorbate have to be described quantum mechanically to achieve convergence for the adsorption energy. The N-Ti bond distance is less sensitive to the interaction with the bridging oxygen atoms and almost converged with one row of bridging oxygens on each side of the adsorbate in the quantum mechanically described subsystem. The Ti_9O_{18} and the $Ti_{40}O_{80}$ cluster provide thus an attractive compromise between accuracy and computational cost for studying the adsorption geometry of small molecules on the TiO_2 (110) surface. Accurate binding energies

can then be obtained from single point calculations on larger clusters. In the present study we used $Ti_{96}O_{192}$ and $Ti_{114}O_{228}$ for HF-SCF and $Ti_{114}O_{228}$ for DFT, which gave a correction of about 7 and 9 kJ/mol, respectively, for the adsorption energy of N_2 in the low coverage limit relative to the result on the $Ti_{40}O_{80}$ cluster. The relaxation of the surface has a large influence on the adsorption energy. It stabilizes the undercoordinated Ti centers on the rutile (110) surface and thereby reduces their reactivity and the adsorption strength. Additionally, our results show that HF-SCF and PBE/DFT are insufficient for accurate adsorption energies of species which interact only weakly with the surface as e.g. N_2. It requires a more balanced treatment of exchange and electron correlation. The B3LYP hybrid functional seems to give reliable adsorption geometries, but for the binding energy even second-order Møller-Plesset perturbation theory gives without spin-component scaling a relatively large error due to the fairly strong correlation effects at the undercoordinated Ti atoms. Only the more robust spin-component scaled version of MP2 and the dispersion corrected B3LYP-D3 give a result for the adsorption energy of N_2 on TiO_2 (110) of -40.9 kJ/mol and -39.2 kJ/mol which agrees reasonable well with the experimental values.

Acknowledgments

The work reported here has been supported by the Deutsche Forschungsgemeinschaft (DFG) through the Collaborative Research Center SFB 558 "Metal-Substrate Interactions in Heterogeneous Catalysis" and its integrated graduate school.

---

[1] U. Diebold, *Surf. SC. Reports* **48**, 53 (2003).

[2] M. A. Nadeem, K. A. Connelly, and H. Idriss, *Int. J. of Nanotechnology* **9**, 121 (2012).

[3] Y. Kuwahara, T. Kamegawa, K. Mori, and H. Yamashita, *Curr. O. Chem.* **14**, 616 (2010).

[4] C. Sun, L.-M. Liu, A. Selloni, G. Q. M. Lu, and S. C. Smith, *J. Mater. Chem.* **20**, 10319 (2010).

[5] F. Rittner, R. Fink, B. Boddenberg, and V. Staemmler, *Phys. Rev. B* **57**, 4160 (1998).

[6] F. Rittner, B. Boddenberg, R. F. Fink, and V. Staemmler, *Langmuir* **15**, 1449 (1999).

[7] L. Maschio, D. Usvyat, F. R. Manby, S. Casassa, C. Pisani, and M. Schütz, *Phys. Rev. B* **76**, 075101 (2007).

[8] M. Marsman, A. Grüneis, J. Paier, and G. Kresse, *J. Chem. Phys.* **130**, 184103 (2009).

[9] G. Sun, J. Kürti, M. Rajczy, P. Kertesz, J. Hafner, and G. Kresse, *Journal of Molecular Structure (Theochem)* **624**, 37 (2003).

[10] A. Grüneis, M. Marsman, and G. Kresse, *J. Chem. Phys.* **133**, 074107 (2010).

[11] T. Bredow, G. Geudtner, and K. Jug, *J. Comp. Chem.* **22**, 89 (2001).

[12] A development of University of Karlsruhe and Forschungszentrum Karlsruhe GmbH, 1989-2007, Turbomole GmbH, since 2007; available from http://www.turbomole.com, *TURBOMOLE V6.3*, 2011.

[13] A. Schäfer, H. Horn, and R. Ahlrichs, *J. Chem. Phys.* **97**, 2571 (1992).

[14] F. Weigend, M. Häser, H. Patzelt, and R. Ahlrichs, *Chem. Phys. Lett.* **294**, 143 (1998).

[15] M. v. Arnim and R. Ahlrichs, *J. Comp. Chem.* **19**, 1746 (1998).

[16] K. Eichkorn, O. Treutler, H. Öhm, M. Häser, and R. Ahlrichs, *Chem. Phys. Lett.* **242**, 652 (1995).

[17] F. Weigend, F. Furche, and R. Ahlrichs, *J. Chem. Phys.* **119**, 12753 (2003).

[18] A. Schäfer, C. Huber, and R. Ahlrichs, *J. Chem. Phys.* **100**, 5829 (1994).

[19] S. Grimme, *J. Chem. Phys.* **118**, 9095 (2003).

[20] C. Hättig, A. Hellweg, and A. Köhn, *Phys. Chem. Chem. Phys.* **8**, 1159 (2006).

[21] C. Hättig, *Phys. Chem. Chem. Phys.* **7**, 59 (2005).

[22] P. A. M. Dirac, *Proc. Royal Soc. (London) A* **123**, 714 (1929).

[23] J. C. Slater, *Phys. Rev.* **81**, 385 (1951).

[24] J. P. Perdew and Y. Wang, *Phys. Rev. B* **45**, 13244 (1992).

[25] J. P. Perdew, K. Burke, and Y. Wang, *Phys. Rev. B* **54**, 16533 (1996).

[26] A. D. Becke, *Phys. Rev. A* **38**, 3098 (1988).

[27] C. Lee, W. Yang, and R. G. Parr, *Phys. Rev. B* **37**, 785 (1988).

[28] A. Becke, *J. Chem. Phys.* **98**, 5648 (1993).

[29] S. Grimme, J. Antony, S. Ehrlich, and H. Krieg, *J. Chem. Phys.* **132**, 154104 (2010).

[30] P. Fuentealba, L. v. Szentpaly, H. Preuss, and H. Stoll, *J. Phys. B.* **18**, 1287 (1985).

[31] R. Restori and D. Scharzenbach, *Acta Cryst. B* **43**, 251 (1987).

[32] K. P. Huber and G. Herzberg, *Constants of Diatomic Molecules*, Van Nostrand-Reinhold, New York, 1979.

[33] A. M. Burow, M. Sierka, J. Döbler, and J. Sauer, *J. Chem. Phys.* **130**, 174710 (2009).

[34] K. N. Kudin and G. E. Scuseria, *Chem. Phys. Lett.* **283**, 61 (1998).

[35] S. C. Ammal and A. Heyden, *J. Chem. Phys.* **133**, 16703 (2010).

[36] P. M. Kowalski, B. Meyer, and D. Marx, *Phys. Rev. B* **79**, 115410 (2009).

[37] J. P. Perdew, K. Burke, and M. Ernzerhof, *Phys. Rev. Lett.* **77**, 3865 (1996).

[38] F. Labat, P. Baranek, and C. Adamo, *J. Chem. Theory Comput.* **4**, 341 (2008).

[39] T. Helgaker, W. Klopper, H. Koch, and J. Noga, *J. Chem. Phys.* **106**, 9639 (1997).

[40] M. Kunat, F. Träger, D. Silber, H. Qiu, Y. Wang, A. C. van Veen, C. Wöll, P. M. Kowalski, B. Meyer, C. Hättig, and D. Marx, *J. Chem. Phys.* **130**, 144703 (2009).

[41] D. N. Furlong, F. Rouquerol, J. Rouquerol, and K. S. W. Sing, *J. Chem. Soc. Faraday Trans.I* **76**, 774 (1980).

[42] Z. Dohnálek, J. Kim, O. Bondrachuk, J. M. White, and B. D. Kay, *J. Phys. Chem. B* **110**, 6229 (2006).

[43] A. Hellweg, S. A. Grün, and C. Hättig, *Phys. Chem. Chem. Phys.* **10**, 1 (2008).

[44] J. Möllmann, S. Ehrlich, R. Tonner, and S. Grimme, *J. Phys: Condens. Matter* (2012), in press.